Marshall Plan Scholarship
Boston, MA; Feb 2011 - Jul 2011
Master curriculum Biomedical Engineering
Vienna University of Technology

Marshall Plan Scholarship Documentation
:: Response of retinal ganglion cells to electric stimulation ::

Paul Werginz,
Wimbergergasse 42/11
A-1070 Vienna
October 31, 2011

Contents

Acknowledgments

First of all I want to thank the 'Marshallplan-Jubilaeumsstiftung' for providing me the financial support to realize my plan of writing my diploma thesis in the USA. This support made it possible to perform a five month research stay at the 'Fried Lab' located at the 'Massachusetts General Hospital' in Boston, MA.

Special thanks go to Dr. Shelley Fried (Massachusetts General Hospital/Harvard Medical School) and Prof. Frank Rattay (Vienna University of Technology) who always helped and motivated me during the process of my thesis. I also want to express gratitude to all members of the 'Fried Lab' who tried to support my work anytime and also let me experience a wonderful time in the USA.

Paul Werginz

1 Introduction

Retinal implants using electric stimulation to activate retinal neurons made large progress in the last two decades. Several groups are working on these kind of prostheses to restore vision to blind people that are suffering of diseases like renitis pigmentosa or macula degeneration. The damage or complete destruction of the photoreceptor layer in the retina leads to a progressive loss of vision. Fortunately the connecting neuronal tissue stays intact and so it is possible to electrically activate these remaining cells. Despite this successful research there are still some major obstacles to overcome. The main problem of electric stimulation in the inner eye is the selective activation of single neurons and connected groups of neurons, respectively. The complex network within the human retina makes it complicated to predict the outcome of external stimulation. It is almost impossible to imitate the different signal processing pathways through the retina. The further progress in this scientific field is influenced by new techniques in nano-fabrication as well as better insight into the physiological function of the retina.

In the field of computational biology mathematical methods are used to describe the behavior of living systems without performing time consuming and expensive experiments. Models which are describing the behavior of neuronal cell membranes are known for over 50 years and help to examine the influence of electric stimulation on neurons. Modern cell membrane models describe the non-linear behavior of ion channel dynamics which are responsible for signal transmission and signal processing in the human body. The combination of physiological experiments and computer simulations allow us to gain better insight into the high sophisticated mechanisms of signal encoding in mammalians. The use of computer simulations also allow us to obtain fast results to support the corresponding experiments.

There are two main approaches of a retinal implant: the sub-retinal implant which is implanted 'under' the retina close to the layer of photoreceptors and the epi-retinal implant which is placed on the 'outside' of the retina close to retinal ganglion cells. In this study we examined how electric stimulation effects the direct activation of retinal ganglion cells. In former studies a specific morphological structure was found within these cells. A band of highly dense sodium channels is supposed to show a particular response to external stimulation.

Because of the morphology of retinal ganglion cells which are combined to the optic nerve it is a problem to activate single neurons and groups of functionally related neurons, respectively. The accidental activation of passing axons from far

away neurons makes it difficult to elicit focal perceptions. The former described structure at the first part of retinal ganglion cells is assumed to give us a possibility to focally activate these neurons.

2 Methods

As starting point for our computational investigations we used the experimentally determined threshold maps from Fried et al. Two major steps had to be performed: First, we had to calculate the electric voltage distributions for a given electrode geometry in a heterogeneous media. Second, we had to build a multi-compartment model to simulate the behavior of a single nerve fiber. Membrane properties were described by a Fohlmeister-Coleman-Miller type model of various ordinary differential equations.

2.1 Finite element calculations

To calculate an electric voltage distribution for an electrode two potential approaches can be used: First, if the medium surrounding the electrode is homogenous and the electrode is modeled as a point source a simple analytic calculation can be computed:

$$V = \frac{\rho_{ext} * I_{stim}}{4 * r * \pi}$$

where ρ_{ext} denotes the external resistance of the electrode embedding media, I_{stim} the stimulating current and r the distance from the electrode.

If the surrounding medium of the electrode is heterogeneous and a real electrode geometry is given the finite element approach leads to more precise results. To optimally imitate the physiological experiments we modeled a two layer model with finite element software (COMSOL Multiphysics, see Fig. 1A). The retina was modeled as a single layer with an isotropic electric resistivity of $60\Omega \cdot cm$, the electrode was embedded in an ames solution which had an isotropic electric resistivity of $110\Omega \cdot cm$. As electrode material we chose (Platinum-Iridium) from the COMSOL Multiphysics material library (electric resistance: $1.05 \cdot 10^{-8}\Omega \cdot cm$), the electrode geometry was the same as used by Fried et al: a cone shaped electrode, $30\mu m$ in base diameter and $35\mu m$ in height. The whole system had the dimension of 1-5x1x1mm to be large enough to avoid edge effects, system boundaries were grounded (V = 0V). To find the same angle between electrode and stimulated tissue that was used in the experiments we performed various calculations for different angles and compared the results (voltage profiles) to the voltage profiles measured experimentally. Calculated results for 10 degrees fitted the data best so all our further simulations were performed with this configuration. The computed voltage profile was exported

to MATLAB and the first ($\frac{dV}{dx}$, electric field) and second ($\frac{d2V}{d2x}$) derivative were calculated.

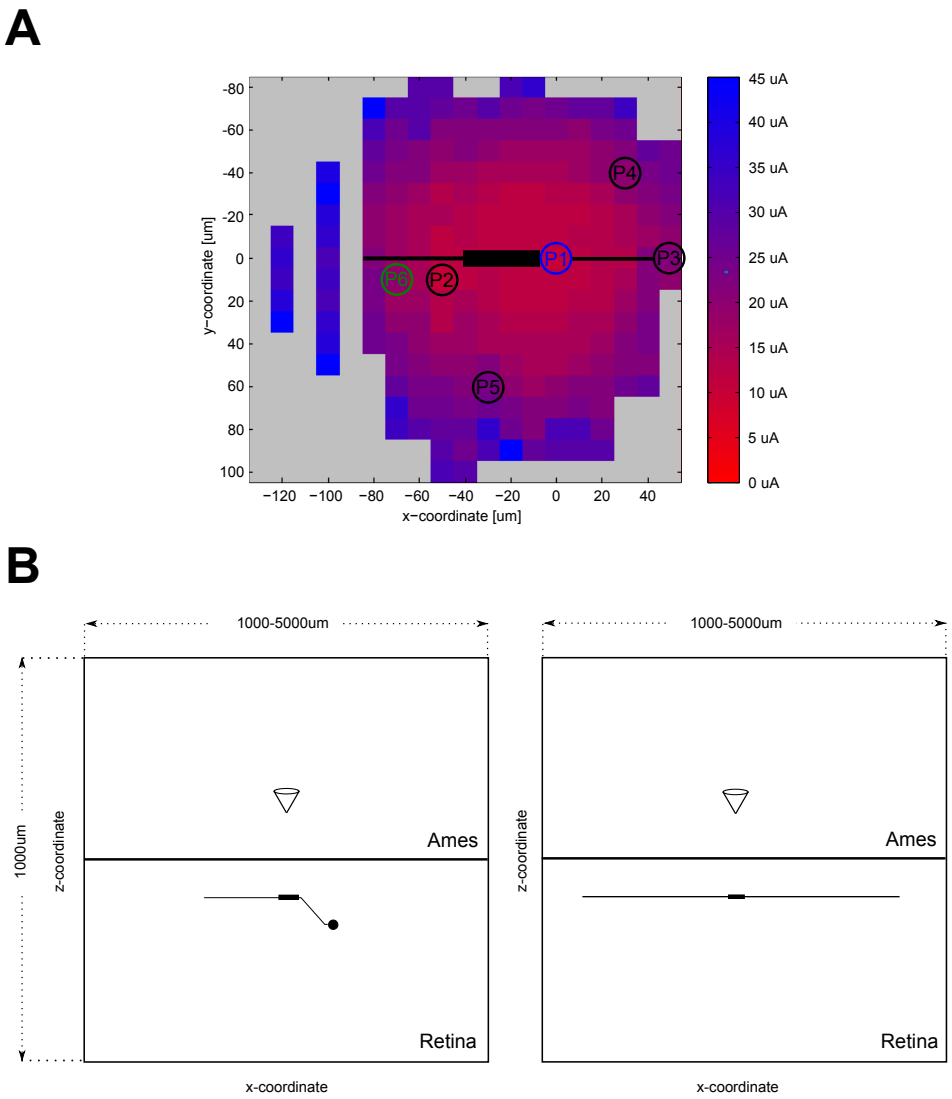

Figure 1: **Location of six electrode positions from threshold map; see table 1 for exact locations and threshold.** (A) A two dimensional colormap shows thresholds for each electrode position. Thresholds vary from $12\mu A$ to ´$45\mu A$ (monophasic, cathodic pulse). The approximate location of the high density sodium channel band is indicated by the thick bar (ref Shelley). The thin horizontal line indicates the approximate position for the axon. (B) Schematic arrangement of the model ganglion cell (left) and a straight axon with a centered band of dense sodium channels (right). The conical stimulating electrode was positioned 30 μm above. The conductivity of the retina, the electrode and Ames solution were different (see text).

2.2 Compartment model & activating function

To investigate the behavior of a modeled nerve fiber we used the method of compartment modeling. The current flow along a stimulated fiber is described by a number

of n compartments with given electrical (membrane) properties. Every compartment is electrically described by a single virtual point in the center at which all electric currents are calculated. Applying Kirchoff's law for compartment n gives following equations:

$$I_{C,n} + I_{ion,n} + I_{axial,n} = 0$$

which further results in:

$$\frac{d(V_{i,n}-V_{e,n})}{dt} \cdot C_{m,n} + I_{ion,n} + \frac{V_{i,n}-V_{i,n-1}}{R_n/2+R_{n-1}/2} + \frac{V_{i,n}-V_{i,n+1}}{R_n/2+R_{n+1}/2} = 0$$

V_i, V_e, R and C_m denote the intracellular potential, applied external voltage, axial resistance and membrane capacity, respectively. With introducing the reduced membrane voltage $V = V_i - V_e$ one is able to deduce the equation to compute the time courses of V_n for every compartment:

$$\frac{dV_n}{dt} = \Big[- I_{ion,n} + \frac{V_{n-1}-V_n}{R_{n-1}/2+R_n/2} + \frac{V_{n+1}-V_n}{R_{n+1}/2+R_n/2} + \frac{V_{e,n-1}-V_{e,n}}{R_{n-1}/2+R_n/2} + \frac{V_{e,n+1}-V_{e,n}}{R_{n+1}/2+R_n/2} \Big] / C_{m,n}$$

The direct stimulating influence of the applied external potential on compartment n is described by the activating function which has the physical unit of [V/s]:

$$f_n = \big[\frac{V_{e,n-1}-V_{e,n}}{R_{n-1}/2+R_n/2} + \frac{V_{e,n+1}-V_{e,n}}{R_{n+1}/2+R_n/2} \big] / C_{m,n}$$

The activating function gives the very first influence of the electric stimulation on the nerve fiber which corresponds to the slope of membrane voltage V_n at stimulus onset. For a point source activating function values are positive within 70◦ from the electrode. Within this region the nerve fiber is depolarized by the external stimulation, parts outside of this region are hyperpolarized.

2.3 Fohlmeister-Coleman-Miller & ion channel dynamics

To simulate the electric properties of the nerve fiber membrane we incorporated ion channel dynamics based on the Fohlmeister-Coleman-Miller model into our model-fiber. These dynamics use various ordinary differential equations to describe the non-linear behavior of nerve fiber membrane. Five currents play an important role within the model: a sodium current (I_{Na}), a calcium current (I_{Ca}) and three types

of potassium currents: a delayed rectifier (I_K), a potassium type A (I_{KA}) and the calcium activated potassium current ($I_{K,Ca}$); additionally a leakage current (I_L) was modeled. The Fohlmeister-Coleman-Miller model shows the same principal characteristics as the famous Hodgkin-Huxley model.

To model a band of highly dense sodium channels we increased the sodium channel conductance in the band region by the 2-30 fold. Corresponding to this increase we also raised the density of the delayed rectifier by the same factor to hold our model fiber in a stable electric state.

2.4 Nerve fiber & temporal parameters

Our model-neuron was a straight fiber with a length of $6000\mu m$ and a diameter of $2\mu m$, the length of the sodium channel band was set to $40\mu m$. Compartment size varied from $5\mu m$ to $20\mu m$ which was small enough to minimize the computational error to the order of 1%. The internal resistance varied from $55\Omega \cdot cm$ to $1100\Omega \cdot cm$, the specific membrane capacity was fixed at $1\mu F/cm^2$. The resting potential was set to -65mV and model temperature was set to 37° Celsius. For stimulation we used a 0.2ms monophasic (cathodic) pulse like in the physiologic experiments. Sodium channel density was held at $70mS/cm^2$ for the axonal parts of the fiber, the band sodium channel density was varied from $140 - 2100mS/cm^2$ (2-30 fold increase).

2.5 Determine thresholds

As criteria for detecting an action potential we looked for a zero-crossing of membrane voltage of at least one compartment within 10ms. When we recorded an action potential the applied stimulus amplitude was taken as threshold level. With this method we were able to draw one- and two-dimensional threshold maps of x-coordinate against threshold, respectively. The compartment which first crossed the 0mV border was taken as site of spike initiation (SSI). This allowed us to determine whether the band region or the axonal part of the neuron was the section where the action potential occurred.

3 Results

3.1 Threshold map

The threshold map in Figure 1A plots the sensitivity to stimulation from a small electrode as it is stepped across the soma and proximal axon regions of a retinal ganglion cell. Each pixel indicates the threshold when the stimulating electrode was positioned at that location. Spacing between adjacent pixels was 10 μm and the electrode height was fixed at a constant distance above the retina (30 μm). The stimulus was a 0.2 ms cathodal pulse (pseudo-monophasic). Under these conditions, measured thresholds ranged from 12-45 μA. Thresholds were lowest in a central region (darkest red) and increased monotonically with distance from the approximate center of this region. The close spatial alignment between the region of lowest threshold and a dense band of voltage-gated sodium channels in the proximal axon, identified immunochemically, suggests that the band is the site of spike initiation in response to extracellular electric stimulation. This is consistent with other physiological studies that showed that such a region was the site of spike initiation in response to synaptic (intracellular) stimulation. If the band is in fact the site of spike initiation in response to extracellular electric stimulation, it is likely that some property of the induced electric field is consistent across the band region for each combination of stimulating electrode location and stimulus level that successfully generated a spike. Our goal here was to determine whether this was the case and if so, what properties of the stimulus and/or the induced field were essential for activation.

Name	x [μm]	y [μm]	Threshold [μA]
P1	00	00	12
P2	-50	10	12
P3	50	00	25
P4	30	-40	22
P5	-30	60	27
P6	-70	10	22

Table 1: **Coordinates and thresholds for six points on threshold map.** z-distance between fiber and electrode is always 30 μm. P1 and P2 are the two points showing lowest threshold on threshold map, P3 represents the soma, P4, P5 and P6 are randomly chosen. All stimuli are cathodic pulses.

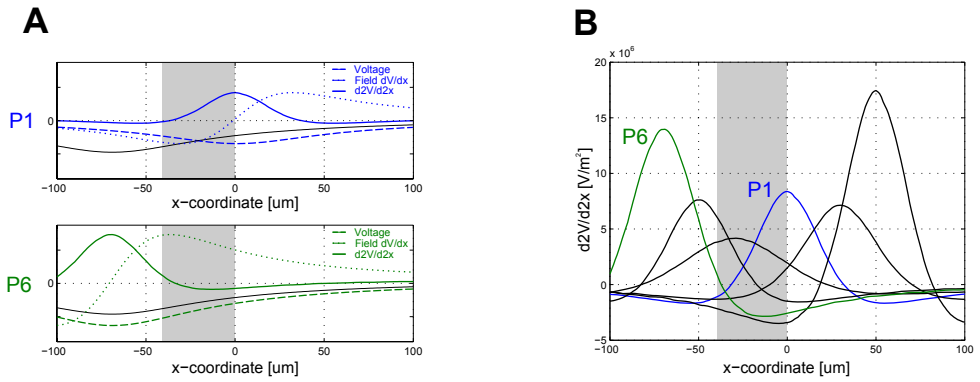

Figure 2: **Some points on the threshold map have a negative activating function in the band region.** (A) Voltage, electric field and derivative of electric field distribution along the axon for points P1 (top) and P6 (bottom). In both panels the 75% voltage profile of P6 is shown (thin black line). Grey shaded region indicates the sodium channel band. (B) Second derivatives for all six points. Note that for some locations of the stimulating electrode, i.e. P6, second derivative is negative within the band region.

3.2 Do one or more components of field underlie activation?

To explore how properties of the stimulus influenced activation of a retinal ganglion cell, we developed a morphologically realistic multi-compartment model of the ganglion cell and then used finite element software (COMSOL Multiphysics) to simulate the effects of stimulation (Methods). The modeled electrode had the same cone-shaped dimensions as the stimulating electrode used in the physiological experiments. The model contained separate layers for the retina and the adjacent Ames solution; impedances of the two layers were 60 and 110 Ω·cm, respectively. Similar to the physiological studies, the distance between the ganglion cell and electrode (z-coordinate) was held fixed at 30 μm.

To explore whether stimulation at threshold generated a consistent effect in and around the band region for different locations of the stimulating electrode, we explored the extracellular voltage generated from six locations of the stimulating electrode within the threshold map of Figure 1A. The x-y coordinates and thresholds for each location are given in Table 1. The points were chosen as follows: points P1 & P2 were the points at which the observed thresholds were lowest, P3 corresponded to the approximate location of the soma, P4, P5 and P6 were chosen randomly across other locations. The one-dimensional spatial profile of extracellular voltage elicited by the stimulus pulse at threshold for two points, P1 and P6, is shown in Figure 2A (dashed red and green lines, respectively). As expected, the peak value of the applied external voltage occurred directly under the stimulating electrode for both locations (0 μm offset for P1; 70 μm offset for P6). While the profiles are

slightly different, it is difficult to ascertain whether one might be more conducive to generation of action potentials. To gain further insight, we reduced the amplitude of the stimulus delivered at P6 to 75% of threshold and plotted the voltage profile from this (reduced amplitude) pulse (thin black line in top and bottom panels). This (reduced) voltage profile had a similar shape and amplitude to the voltage profile arising from threshold stimulation at location P1. However, the profile from location P1 resulted in an action potential while the (reduced) profile arising from location P6 did not. This suggests that the applied external voltage profile across the band by itself does not underlie spike initiation. The one-dimensional electric field of each voltage profile was calculated by taking the derivative of the external voltage along the x-coordinate of the fiber ($\frac{dV}{dx}$). The electric fields across the band arising from threshold stimulation at locations P1 and P6 (red and green dotted lines, respectively) showed little similarity, suggesting that the field is also not the key component underlying action potential initiation.

Because much previous work with axonal stimulation indicates that the activating function is a good predictor for the site of spike initiation we approximated the activating function arising from threshold stimulation at each location by calculating the second derivative of the external voltage ($\frac{d2V}{d2x}$) (Methods) arising from stimulation at each location (green and red solid lines). Surprisingly, the second derivatives of the voltage profile arising from stimulation at the six locations also revealed no apparent similarities in and around the band region (Fig. 2B). For example, the second derivative profile across the band region was completely positive for stimulation arising from some locations (i.e. P1) but completely negative for stimulation arising from other locations (i.e. P6). Because a negative second derivative suggests that the band's initial response to stimulation will be hyperpolarization, these results bring into question whether the band is actually the site of spike initiation for all stimulus locations.

3.3 Activation of a uniform fiber

Because the lack of consistency across the band regions, especially for the second derivative profiles, was in contrast to many previous studies involving stimulation of uniform axons, we considered the possibility that the complex morphology of the ganglion cell was influencing our results. Therefore, we restricted the next round of simulations to a uniform axon fiber model (Fig. 1B, right) (Methods). The modeled fiber had a uniform diameter of 2 μm and a length of 6 mm that was subdivided

into 601 compartments each 10 μm in length. A 40 μm long band of voltage-gated sodium channels was modeled in the center of the axon by increasing the sodium channel conductance in the five center-most compartments; conductance in these five compartments was increased to range from 2-30 times the conductance in the rest of the axon. The dynamics of the voltage-gated ion channels in the cell membrane were adapted from Fohlmeister et al (Methods). With a band conductance of 2100 mS/cm^2 (corresponds to a 30-fold increase of sodium channel density with respect to the rest of the axon), thresholds for the model fiber ranged from 45-98 μA. This range is comparable to but slightly larger than the actual thresholds measured physiologically (Fig. 1A). In agreement with previous studies, compartments with the largest activating functions were the site of spike initiation (not shown).

Because the activating function is a static measurement, i.e. it applies only to the time period immediately following pulse onset, we examined the dynamics of individual compartments during the 0.2 ms duration of the pulse and found that the width of the depolarized region broadened throughout the duration of the pulse (Fig. 3B, t=0.2 ms). This widening can be thought of as a spread of positive charge from the central regions to the negatively charged regions immediately adjacent. Thus there were three different categories of response that arose in individual compartments (Fig. 3C). First, some compartments had a positive activating function and remained depolarized throughout the duration of the pulse. These were typically the compartments closest to the site of stimulation (labeled as '++' in Figure 3C). Second, some compartments had negative activating functions and remained hyperpolarized throughout the pulse (labeled as '$--$'). Finally, some compartments hyperpolarized at pulse onset (negative activating function) but depolarized during the course of the pulse (labeled as '$-+$'). We calculated the extent of these 3 regions for stimulation from location P1 (Fig. 3D). Compartments with a positive activating function were constrained within the two innermost vertical lines during the course of the 2 ms pulse. The extent of the compartments that were depolarized expands to incorporate the region between the two outermost vertical lines (Fig. 3D). The time course of the compartments shown in Fig. 3C correspond to x locations of 0, 50 and 200 μm in Figure 3D. The inset at the top left of Figure 3C shows the response to stimulation immediately following pulse onset (activating function) for each type of response. We plotted membrane voltage at the end of the pulse for all six stimulating electrode locations and found that now all compartments within the band were depolarized (Fig. 3E). This suggests the possibility that band regions that initially hyperpolarize might still initiate spikes.

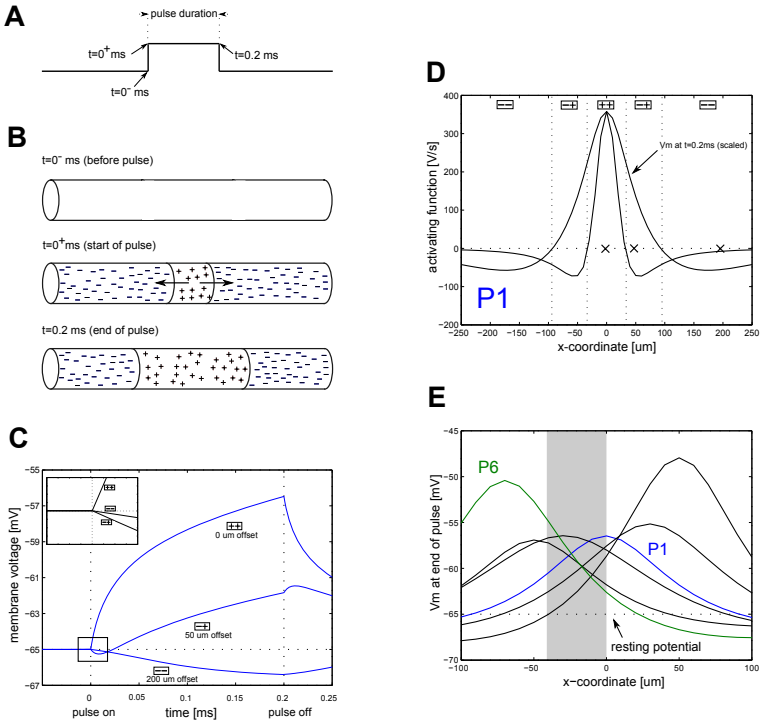

Figure 3: **Some compartments with negative activating functions are depolarized at end of pulse.** (A) Time course of the applied pulse over time. (B) The depolarized region gets broader over time due to the flow of balancing currents. (C) Membrane voltage versus time for the three different compartments (X's in panel D). In the ++ area all compartments have positive activating functions and membrane voltages after pulse ending are positive. Compartments in the $-+$ region have a negative activating function but are depolarized by the end of the pulse. Both, activating function and membrane voltage, are negative in the $--$ region. Stimulating pulse onset at t = 0ms and offset at t = 0.2ms. (D) Activating function and membrane voltage (scaled) at end of pulse (0.2ms pulse duration) for location P1. The region indicated by ++ has a positive activating function and Vm (membrane voltage) remains positive. The region indicated by $-+$ has a negative activating function but Vm is positive at end of the pulse. The region indicated by $--$ has a negative activating function and Vm remains negative. Three 'x's indicate compartments centered at 0μm, 50μm and 200μm offset (see panel C). (E) Membrane voltage at the end of the pulse for the six locations of the threshold-map depicted in Fig. 1. Note that in contrast to Figure 2B all compartments in the band region are now depolarized (resting potential > -65mV).

3.4 The presence of a band alters the expected site of spike initiation

To explore under which conditions this might occur, we incorporated a sodium channel band into the uniform axon (Fig. 4A) and compared the response of the axon with band to that of the original uniform axon. The density of the sodium channels in the band varied from 140-2100 mS/cm^2; 2-30x (respectively) the density of sodium channels in the rest of the axon (and in the uniform fiber). All other properties of the two fibers were identical. Initial simulations compared the response to stimulation from a point source located 50 um from the fiber center (Fig. 4B).

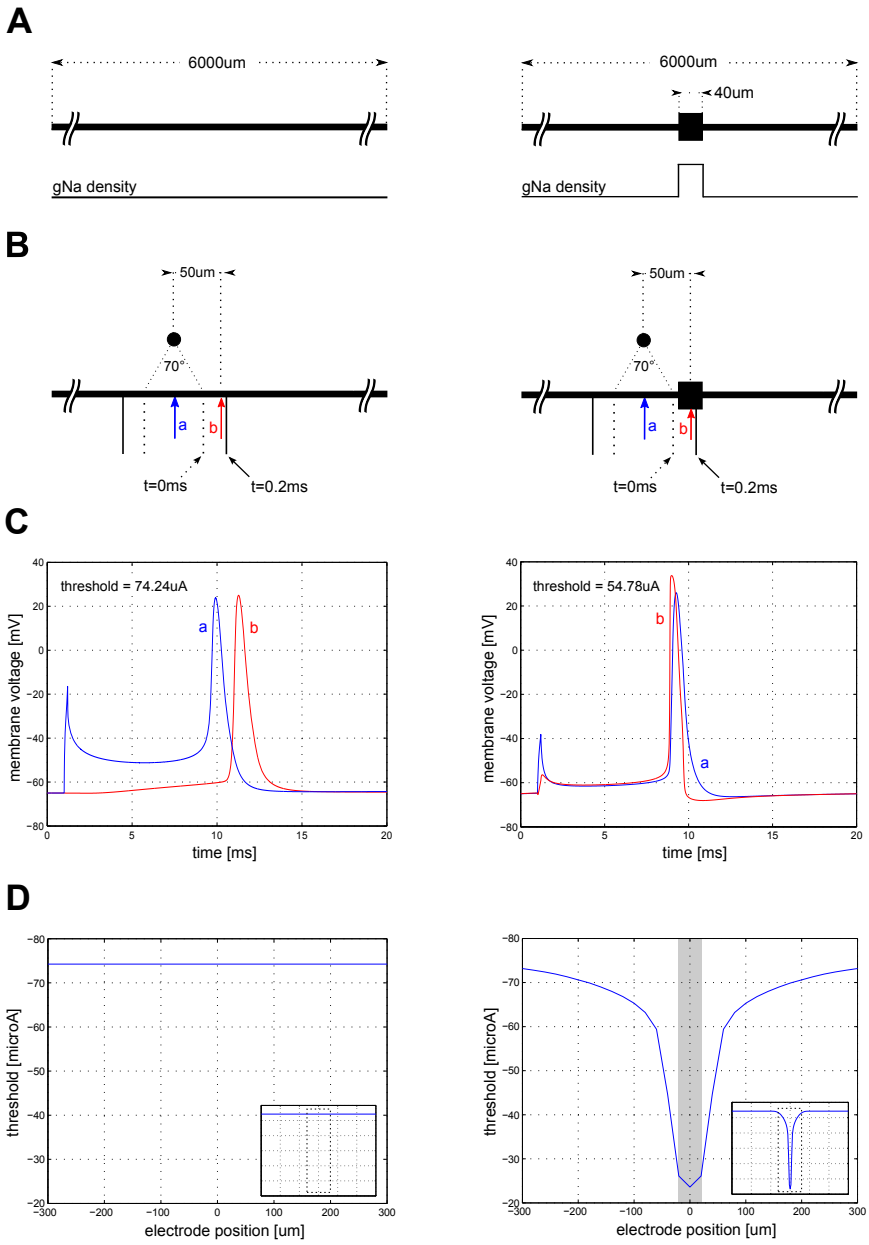

Figure 4: **A band of high density sodium channels influences the site of spike initiation.** (A) Comparison of two different biophysical structures: A straight uniform axon without (left) and with (right) a centered high density band of voltage gated sodium channels. (B) The circle depicts a point source stimulating both structures at the same relative position. Dotted lines and arrows at the bottom indicate the border between depolarization and hyperpolarization regions for activating function (t = 0ms); solid vertical lines indicate membrane voltage at pulse offset (t = 0.2ms) (see Figures 3A and B). (C) Membrane voltage vs. time for two compartments: The red curve ('b') indicates response of the center-compartment whereas the compartment corresponding to the blue trace ('a') is located directly under the electrode. Stimulus amplitude is set to threshold level on both sides. (D) Threshold level for different electrode positions along fiber shows a threshold decrease that extends far beyond the actual band.

The compartments corresponding to a region subtended by a 70 degree angle from the point source had a positive activating function and depolarized initially in

response to the stimulus pulse. The extent of the 'subtended' region is indicated by the two inner dotted vertical lines below the fiber in Figure 4B; the inner line on the right is labeled as 't=0 ms'. As described in Figure 3, the portion of the axon that was depolarized expanded during the course of the pulse – the range of this expansion is indicated by the two outer solid vertical lines, the outer-most of which is labeled 't=0.2 ms'.

We examined the response to stimulation over time in two analogous compartments from each fiber: the first compartment was located directly below the point source and was 50 μm from the fiber center while the second was located at the center of the fiber (Fig. 4C, blue and red traces respectively). The first compartment corresponded to a '$-+$' region (Fig. 3), i.e. a compartment that hyperpolarized initially but was depolarized by the end of the pulse. As expected spike initiation in the uniform fiber occurred directly below the point source (left panel). The triggered spike propagated along the fiber and was observed at the fiber center a short while later (Fig. 4C, left). Surprisingly however, in the fiber with the band, the spike in the band region was initiated prior to the spike in the compartment directly below the point source (Fig. 4C, right). This occurred even though the activating function was negative in this compartment. The threshold for the fiber with the band was less than that for the uniform fiber, most likely because of the higher sodium channel conductivity.

We computed one-dimensional threshold maps for both fibers to explore how the presence of the band influences threshold. When a stimulating electrode was stepped along the axis of the uniform fiber the thresholds remained constant regardless of the position of the stimulating electrode (Fig. 4D, left). For the fiber with the sodium channel band, threshold was lowest when the stimulating electrode was over the fiber center (the band) and increased monotonically for movement away from center (Fig. 4D, right). Thresholds reached a value within 1% of that for the uniform axon at a distance of 800 μm from fiber center (not shown); we refer to this distance as the border in subsequent analysis.

To test the extent of band influence on the site of spike initiation, we moved the point source to 1000 μm from the fiber center and repeated the simulation described above (Fig. 5). For this case, the compartment below the fiber center remained hyperpolarized throughout the stimulus ('$--$'). Surprisingly however, the compartment at fiber center was still the site at which spiking was first initiated (Fig. 5C). This strongly suggests that the properties of the band modulate the site of spike initiation strongly enough to outweigh the influence of the initial depolarization, i.e.

the site predicted by the activating function.

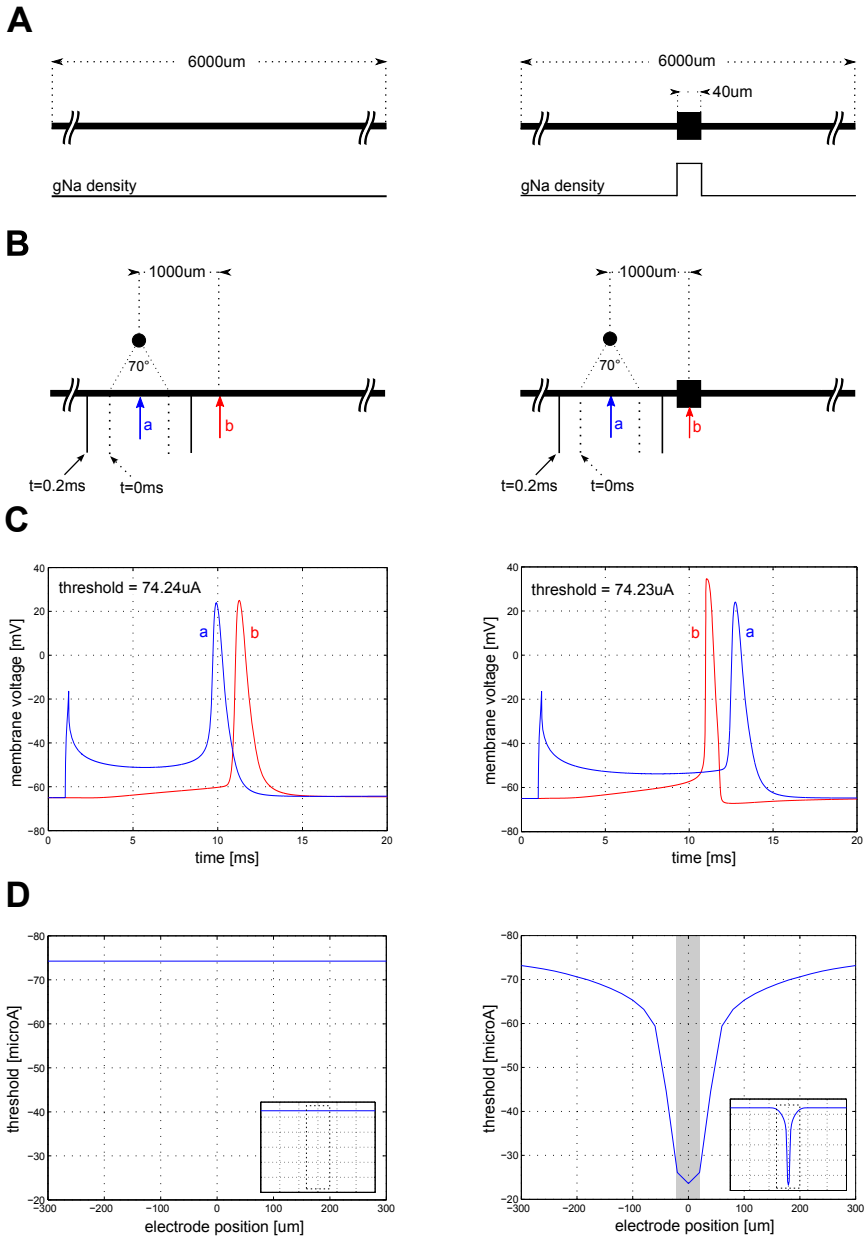

Figure 5: **A band of high density sodium channels influences the site of spike initiation.** (A) Comparison of two different biophysical structures: A straight uniform axon without (left) and with (right) a centered high density band of voltage gated sodium channels. (B) The circle depicts a point source stimulating both structures at the same relative position. Dotted lines and arrows at the bottom indicate the border between depolarization and hyperpolarization regions for activating function (t = 0ms); solid vertical lines indicate membrane voltage at pulse offset (t = 0.2ms) (see Figures 3A and B). (C) Membrane voltage vs. time for two compartments: The red curve ('b') indicates response of the center-compartment whereas the compartment corresponding to the blue trace ('a') is located directly under the electrode. Stimulus amplitude is set to threshold level on both sides. (D) Threshold level for different electrode positions along fiber shows a threshold decrease that extends far beyond the actual band.

To further explore the influence of the band on the site of spike initiation, we

determined the threshold 'borderline' as the site of spike initiation was shifted from the band to the distal axon; the borderline refers to the location where the difference in thresholds between the site of lowest threshold and the distal axon was reduced below 1%. As expected this border was highly sensitive to the biophysical properties of the axon, e.g. internal resistance and ion channel densities. Increasing the internal resistance and/or lowering the sodium channel density narrowed the region in which thresholds were lowest (Fig. 6).

A higher internal resistance led to smaller axial currents which reduce the effect of the passive current propagation along the fiber and consequently axon threshold increases in the axon. A five-fold increase in internal resistance (22 to 110 Ω·cm) resulted in an increase in axonal threshold from 35 to 47 μA (Fig. 6A). A decrease in sodium channel density within the band decreased the influence because the threshold for spike initiation increased. Increasing the sodium channel density within the band to twice that of the rest of the axon resulted in a minimum threshold of 35.5 μA whereas a thirty fold increase in sodium channel density resulted in a minimum threshold of 16 μA (Fig. 6B). Both ratios of axon to band sodium channel density (2:1 and 30:1) resulted in the same threshold in regions far from the band.

3.5 Gaussian shaped voltage profiles

For a better understanding of the mechanisms that lead to an action potential generation we started to apply external voltage profiles which had the shape of Gaussian curves. σ^2 was varied to see the influence of different widths of the voltage distributions (Fig. 7A) and the corresponding first (Fig. 7B) and second (Fig. 7C) derivatives. We calculated thresholds for four different fiber configurations (sodium channel density and ratio was varied) (Fig. 7D). The scaling factor K was the multiplication factor for the probability distribution function (= applied gaussian curve). Lower σ^2 which correspond to sharper voltage distributions showed lower thresholds whereas broader voltage profiles resulted in higher K values. We also plotted the peak of the applied gaussian voltage profile against sigma2 at threshold level (Fig. 7E & Fig. 7F). A simple uniform axon (axon to band sodium channel density ratio = 1:1) showed the lowest peak value for a $\sigma^2 = 1000$ whereas for an axon with an incorporated band we observed lowest peak values at $\sigma^2 = 400$ (Fig. 7F).

Doubling and halving length of the sodium channel band (20um, 40um, 80um band length) showed similarities in the region of lowest peak values of the Gaussian

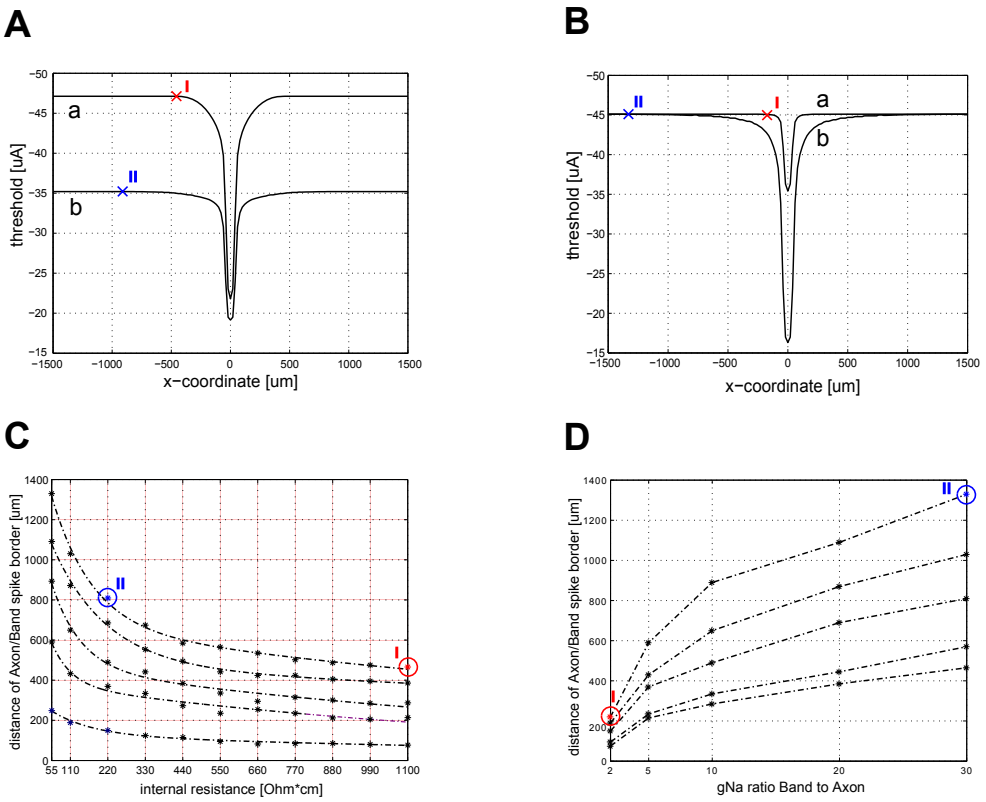

Figure 6: **Band parameters strongly influence the site of spike initiation.** (A) One-dimensional threshold map for internal resistances of $1100\Omega \cdot cm$ (a) and $220\Omega \cdot cm$ (b). Red and blue crosses indicate begin of region where threshold varies by less than $0.01\mu A$. (B) Threshold map for sodium channel density (gNa) ratios between band and axon of $2:1$ (a) and $30:1$ (b). Again, red and blue crosses indicate begin of region where threshold varies by less than $0.01\mu A$. (C) Plots of internal resistance versus the location where threshold varies by less than $0.01\mu A$ for five different gNa ratios between band and axon (2:1, 5:1 10:1 20:1 30:1). The points labeled 'I' and 'II' correspond to 'I' and 'II' in panel (A). Exponential curves are fitted to calculated data. (D) Plots of gNa ratio between band and axon versus points where threshold varies by less than $0.01\mu A$ for five different internal resistances $(55, 110, 220, 550, 1100\Omega \cdot cm)$. The points labeled 'I' and 'II' correspond to 'I' and 'II' in panel (B).

curve but different thresholds for broad voltage profiles (Fig. 8A). The minimum for all three curves was observed at sigma2=400. For a fixed band sodium channel density (350mS/cm2) and three different ratios (10:1, 5:1, 2.5:1) results also showed almost no differences within the minimum region which was again around σ^2=400 (Fig. 8B).

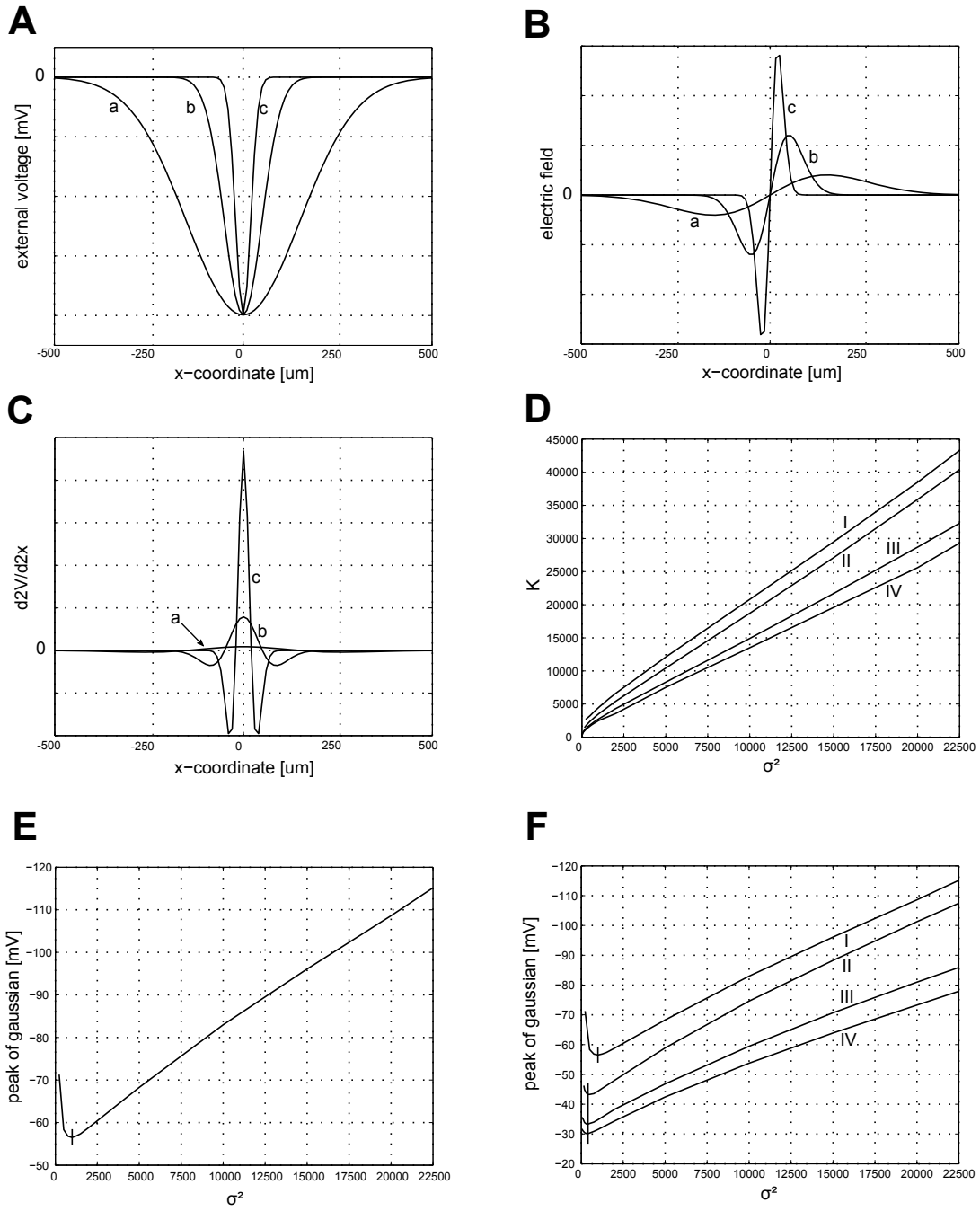

Figure 7: **Different gaussian voltage profiles change the response of the high density sodium channel band.** (A,B,C) Three different gaussian voltage profiles (A) and their first ((B), i.e. electric field) and second ((C), i.e. d2V/d2x) derivatives. (a) corresponds to σ^2=22500, (b) σ^2=2500 and (c) σ^2=400. (D) Plots of σ^2 versus the scaling factor K at threshold for different band/axon-configurations. (I): Uniform sodium channel density of $70mS/cm^2$. (II): Band sodium channel density of $150mS/cm^2$ and axon sodium channel density of $30mS/cm^2$ (ratio 5:1). (III): Band sodium channel density of $350mS/cm^2$ and axon sodium channel density of $70mS/cm^2$ (ratio 5:1). (IV): Band sodium channel density of $500mS/cm^2$ and axon sodium channel density of $100mS/cm^2$ (ratio 5:1). (E) Plot of σ^2 versus the peak of the applied gaussian voltage profile for a straight uniform axon. The lowest gaussian peak value (vertical line) corresponds to a σ^2 of 1000. (F) Plots of σ^2 versus the peak of the applied gaussian voltage profiles. Labels (I,II,II,IV) correspond to the four configurations in (D). The two vertical lines show the minimum for every curve.

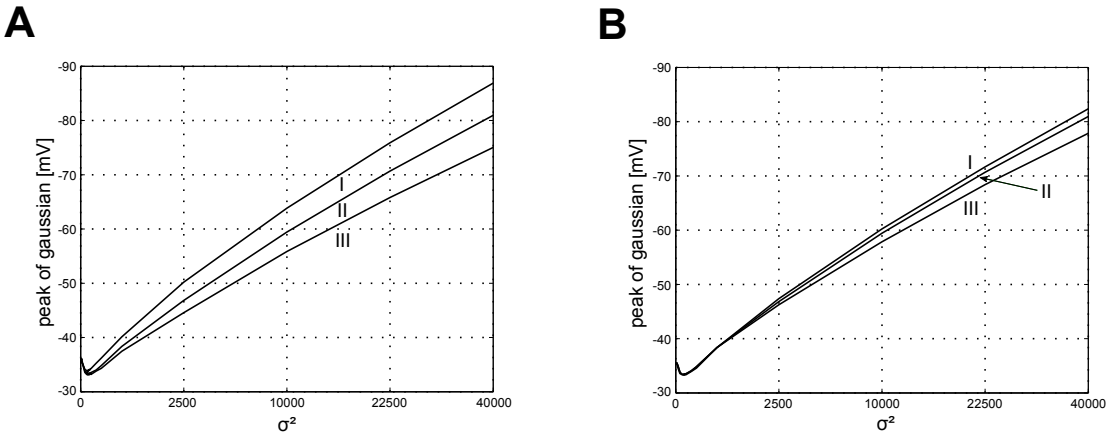

Figure 8: **Band parameters influence the response to voltage gaussian profiles.** (A) Plots of σ^2 versus the threshold level (peak of the applied gaussian profile) for three different band lengths ($20\mu m$ (a), $40\mu m$ (b), $80\mu m$ (c)). (B) Plots for three different ratios of the band to axon sodium channel density (10:1 (a), 5:1 (b), 2.5:1 (c)), band sodium channel density is fixed at $350mS/cm^2$.